Mercury records covering the past 90 kyr from lakes Prespa and Ohrid, SE Europe

Alice R. Paine[1*], Isabel M. Fendley[1], Joost Frieling[1], Tamsin A. Mather[1], Jack H. Lacey[2], Bernd Wagner[3], Stuart A. Robinson[1], David M. Pyle[1], Alexander Francke[4], Theodore R Them II[5], Konstantinos Panagiotopoulos[3]

[1]Department of Earth Sciences, University of Oxford, UK, OX1 3AN
[2]National Environmental Isotope Facility, British Geological Survey, Nottingham, UK
[3]Institute of Geology and Mineralogy, University of Cologne, Cologne, Germany
[4] School of Physics, Chemistry & Earth Science, Faculty of Science, Engineering & Technology, The University of Adelaide, Adelaide, Australia
[5]Department of Geology and Environmental Geosciences, College of Charleston, Charleston, SC 29424, USA
*Corresponding Author: alice.paine@earth.ox.ac.uk

SUPPLEMENTARY INFORMATION

Text SI1: Lake Prespa coring details

Three sediment cores of >1m length (Co1204, Co1215, Co1216) were recovered from Lake Prespa in 2007 and 2009 using a floating platform (Wagner et al., 2012). A gravity corer was used for undisturbed surface sediments, and a 3-m-long percussion piston corer (UWITEC Co. Austria) was used for deeper sediments. This study presents data for core Co1215 (40°57 N, 20°58 E), which was recovered from the central northern part of the lake, with a measured water depth of 14.5 m at the time of extraction (October 2009), and hydroacoustic surveys displaying relatively undisturbed sedimentation (Wagner et al., 2012). With a total length of 17.76 m, core Co1215 was cut into segments of up to 1 m length following recovery, and stored in the dark at 4°C until further processing. One core half was used for non-destructive analyses (e.g., XRF scanning) and then archived at the Institute of Geology and Mineralogy at the University of Cologne, Germany. The other half was subsampled at 2 cm intervals and the samples were freeze-dried and homogenized using an agate ball mill (Panagiotopoulos et al., 2014).

Text SI2: Lake Ohrid coring details

The DEEP site (5045-1) is the main drill site in the central part of the lake (Francke et al., 2016; Wagner et al., 2019), and this study presents data for the upper 36.27 m of the sequence. Water depth at this site is ~243m. The uppermost sediments at the DEEP site down to 1.5 m below lake floor (b.l.f.) were recovered in 2011 using a UWITEC gravity and piston corer (core Co1261). In 2013, sediments below 1.5 m were cumulatively recovered from six different drill holes (5045-1A to 5045-1F) at the DEEP site, with the distance between each drill hole averaging ~40 m. Holes 5045-1A and

5045-1E comprise sub-surface sediments down to ~2.4 and 5m, respectively. Holes 5045-1B and 5045-1C were drilled to a maximum depth of 480m, and hole 5045-1D down to 569 m. Spot coring down to 550m was conducted in hole 5045-1F to fill any gaps present in the other holes (Wagner et al., 2014). During the drilling campaign in 2013, onsite core processing comprised smear-slide analyses of core catcher material and magnetic susceptibility measurements on the whole cores in 2 cm resolution using a Multi-Sensor Core Logger (MSCL, GEOTEK Co.) equipped with a Bartington MS2C loop sensor (Francke et al., 2016).

Following the field campaign, the cores were shipped to the University of Cologne cut in (up to) 1m long segments following core recovery, and stored in darkness at 4°C. (see also Wagner et al., 2014). First correlation of the individual core segments was established based on the magnetic susceptibility data of the whole cores from holes 5045-1B, 5045-1C, 5045-1D, and 5045-1F. Cores incorporated into the composite profile were then split lengthwise and described for colour, grain size, structure, macroscopic components, and calcite content. If an unequivocal core correlation was not possible, additional core sections from other drill holes in the respective depths were opened, likewise analyzed, and used to refine the core correlation (Francke et al., 2016).

Text SI3: Lake Prespa chronological details

A chronology for Co1215 was produced by Damaschke et al. (2013), using linear interpolation between 29 discrete tie points dated using ^{14}C or electron spin resonance (ESR). Here, we update this chronology using the same tie-points (**Table S1**), along with the rBacon v 2.5.7 (Blaauw and Christeny, 2011) Bayesian age-depth modelling package to account for the newest (IntCal2020) radiocarbon calibration. The rBacon package combines the dates and uncertainty of specific horizons with prior information – an initial assumption of sedimentation rate, as well as the principle of superposition (age must increase with depth). Bacon subdivides the core into many individual segments which each have a uniform sedimentation rate; in this case we have chosen a segment length of 10 cm. Markov Chain Monte Carlo (MCMC) iterations are subsequently performed, each calculating a sedimentation rate for each segment of the entire record.

The revised model integrates updated ^{40}Ar/^{39}Ar dates of eruptions geochemically correlated to specific tephra layers within the Prespa core (Damaschke et al., 2013); such as the Y-5 (39.35 ± 0.11 ka (Giaccio et al., 2017)) and Y-6 (45.5 ± 1 ka (Zanchetta et al., 2018)) tephra units (**Table S1**). Tephra layers are assumed to have been deposited instantaneously. The ^{14}C ages and tephra ages and their respective uncertainties are incorporated as tie-points, and were calibrated using IntCal20 (Reimer et al., 2020) in rBacon simultaneous with age-depth model creation. One exception to this is the Y-3 tephra layer, which was assigned a date adapted from Wulf et al., (2018). This study used Bayesian age-depth modelling (OxCal v. 4.3) (Ramsey, 2009) to estimate the age of the Y-3 unit, following identification of the tephra layer in both the Tenaghi-Philippon and Lago Grande di Monticchio terrestrial sediment records, alongside marine cores from the Ionian, Tyrrhenian, and Adriatic seas (Bronk Ramsey et al., 2015; Albert et al., 2015). We re-calibrated the date to IntCal20 by re-running

the OxCal code from (Wulf et al., 2018), and updating the curve to IntCal20 and Marine20 for the terrestrial and marine sections respectively (from IntCal13/Marine13). We did not change the Delta (Δ)^{14}C parameter for the marine localities. The cal. ka BP age for the Y-3 from Wulf et al., (2018) was 29.059 ± 0.356, and our updated date is 28.881 ± 0.314 (± 2σ), so a total difference of only ~200 years.

Table S1: Details of the eleven tephra layers identified in Co1215 (Damaschke et al., 2013). Visible tephra layers are described with bold text, and M refers to eruption magnitude.

Unit (Co1215 ID)	Core Depth (m)	Thickness (cm)	Source	M	Tephra Composition	Mean Glass SiO$_2$ (%)
512 AD (PT0915-1)	0.554 – 0.556	0.2	Somma-Vesuvius	4.0	Phonolite	48.6
Mercato (PT0915-2)	**1.556 – 1.562**	**0.6**	**Somma-Vesuvius**	**6.1**	**Phonolite**	**58.34**
LN1 (PT0915-3)	2.65 – 2.67	0.2	Campi Flegrei	N/A	Trachyte	61.3
LN2 (PT0915-4)	2.87 – 2.89	0.2	Campi Flegrei	N/A	Trachyte	61.07
Y-3 (PT0915-5)	**6.168 – 6.178**	**1**	**Campi Flegrei**	**6.0**	**Trachyte**	**60.9**
Unknown (PT0915-6)	**6.90 – 6.932**	**3.2**	**Unknown**	**N/A**	**N/A**	**57.3**
Y-5 (PT0915-7)	**7.648-7.838**	**19**	**Campi Flegrei**	**7.7-7.8**	**Trachyte**	**60.3**
SMP1-a (PT0915-8)	8.42-8.44	0.2	Ischia	6.0	Phonolite	60.6
Y-6/Green Tuff (PT0915-9)	**8.54 – 8.56**	**2**	**Pantelleria**	**6.4**	**Trachyte**	**71.13**
Unknown (PT0915-10)	9.008 – 9.01	0.2	Unknown	N/A	N/A	60.8
Unit C (PT0915-11)	**10.786 – 10.796**	**1**	**Etna?**	**N/A**	**Basalt**	**60.8**

Table S2: Tie-points used in generation of a Bayesian age model for core Co1215 from Lake Prespa

Lab ID	^{14}C uncal. (yr)	Error (2σ)	Error (1σ)	Core Depth (cm)	Description	Technique	Ref.
ETH-40050	-1190		30	5	SF	^{14}C	1
Col1030	715		28	43	PR	^{14}C	1
ETH-40052	3095		35	75	BOM	^{14}C	1
ETH-40051	2080		35	75	PR	^{14}C	1
Col1031	6003		28	106	BOM	^{14}C	1
ETH-40054	7055		40	129	BOM	^{14}C	1
ETH-40055	8205		40	146.5	BOM	^{14}C	1
ETH-40057	9090		35	167	BOM	^{14}C	1
ETH-40056	8755		35	167	PR	^{14}C	1
ETH-40059	9840		35	185	BOM	^{14}C	1
ETH-40060	10837		132	213	FR	^{14}C	1
ETH-40063	11005		40	215	BOM	^{14}C	1
ETH-40062	11466		121	215	FR	^{14}C	1
Col1032	14056		71	302	PR	^{14}C	1
ETH-40065	33075		210	728.5	PR	^{14}C	1
ETH-40064	26345		105	634	PR	^{14}C	1
KIA-36356	33270	540		825	PR	^{14}C	2
KIA-36357	37960	570		875	PR	^{14}C	2
Visible tephra							
PT0915-7	39850	140	70	774.3	Y-5 (Campi Flegrei)	^{40}Ar/^{39}Ar	3
PT0915-7	34290		90	774.3	Y-5 (Campi Flegrei)	^{14}C	3
PT0915-9	45500	1000	500	855	Y-6 (Pantelleria)	^{40}Ar/^{39}Ar	4,5
PT0915-2	7770		40	155.9	Mercato (Somma-Vesuvius)	^{14}C	7,8
PT0915-5	28881.5	316.5	158.25	617.3	Y-3 (Campi Flegrei)	Bayesian	9
PT0915-1	1438	1	0.5	55.5	512 AD (Somma-Vesuvius)	^{14}C	1
PT0915-3	12600		110	266	LN1	^{14}C (foram)	10
PT0915-4	12870		100	288	LN2	^{14}C (foram)	10
Non-radiocarbon							
K-5800	73900		9900	1460.5	CSF	ESR	1
K-5835a	68900		5100	1479	CSF	ESR	1
K-5836a	84100		7800	1464	CSF	ESR	1

1 – Damaschke et al. (2013); 2 – Wagner et al. (2012); 3 – Giaccio et al. (2017); 4 - Scaillet et al. (2013); 5 - Zanchetta et al. (2018); 6 - Zanchetta et al. (2011); 7 – Tomlinson et al. (2015); 8 – Vogel et al. (2010); 9 - Wulf et al. (2018); 10 – Siani et al. (2004)

BOM – bulk organic matter; FR – fish remains; PR – plant remains; SF – shell fragments (*Dreissena presbensis*); CSF – shell fragments (Carino mussel); ESR – electron spin resonance

The final age-depth model used in this study is the median of all the iterations generated by rBacon, which is generally indistinguishable from the mean. The upper 2 m (Holocene) section is constrained using 10 radiocarbon dates and 2 tephras/cryptotephra layers as tie-points, with age uncertainties in

this section ranging from ~5 years just below the surface, to ~580 years between 1.5 – 2 m. Uncertainties increase with depth, with basal sediments showing uncertainties of up to ~7550 years. This can be attributed to significantly fewer independent chronological anchors available in this core section, with three ESR dates providing the only currently available tie points below 10.66 m depth.

Our revised model shows broad agreement with the interpolation-based chronology presented by Damaschke et al., (2013), and confirms that core Co1215 provides a continuous record of sedimentation over the past 89.9 ka (**Fig. S1**). Age differences generally do not exceed ~2-kyr at any given depth. One exception is seen between 9.93 and 11.92 m, where our model generates ages up to ~4.9-kyr younger than those generated by Damaschke et al. (2013) (**Fig. S1**). Given that no additional tie points were added in generation of the revised model, this difference is likely due to refinements made to the IntCal2020 radiocarbon calibration for dates prior to 30 ka (Reimer et al., 2020). Specifically, incorporation of speleothem-derived U-Th data from China (Cheng et al., 2016), revision of varved lake sediment chronologies (e.g., Lake Suigetsu, Japan (Staff et al., 2013), and inclusion of new marine sediment records (e.g., Cariaco Basin - (Hughen and Heaton, 2020)) has permitted a curve extension to ~54 ka. This not only provides more accurate age estimations for the Late Pleistocene than was possible for IntCal09 (the calibration used in the 2013 model; (Reimer et al., 2009)), but also yields millennia-scale age differences >40 ka between calibrations. For example, calibrated ages are found to be up to ~2-kyr younger in IntCal20 compared to IntCal13 (Reimer et al., 2020). Increasingly younger ages in each successive iteration of the IntCal curve beyond 30 ka implies an >2-kyr age difference between IntCal09 and IntCal20, which is consistent with the differences observed between the two age models for Co1215.
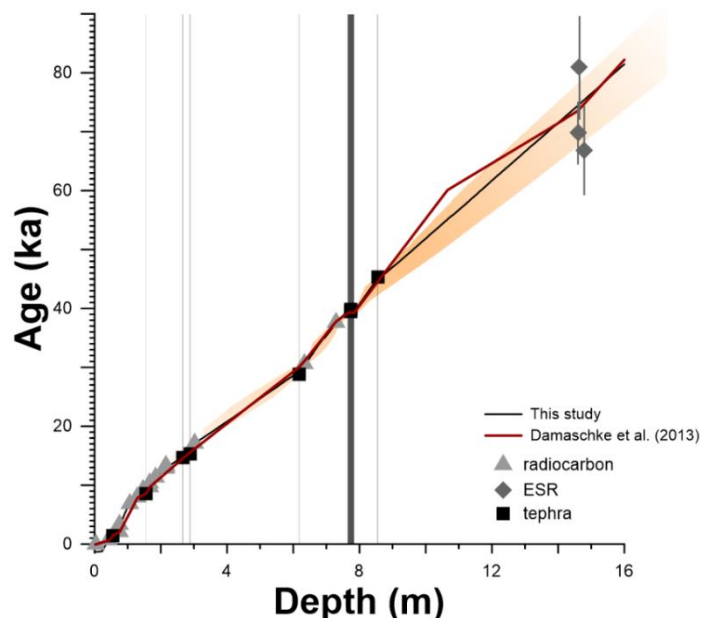
Figure S1: An updated Bayesian age-depth model for core Co1215 from Lake Prespa (*this study* – black line), compared to the age model presented in Damaschke et al. (2013) (red line). Calibrated ages for the twenty-seven tie points used in model generation are displayed by type: radiocarbon-dated bulk organic, fish, or aquatic plant remains (light grey triangles), volcanic tephra layers (black squares) and electron-spin resonance-derived dates for a shell layer (*Dreissena*) located at 14.63–14.58 m depth (dark grey diamonds). Uncertainties for ESR dates at 1σ are presented as pink vertical lines. Uncertainties for radiocarbon and tephra dates are within the displayed point sizes. Minimum and maximum model ages at

95% (2σ) confidence are marked with orange shading. Grey bars mark the stratigraphic placement of tephra layers used as tie-points, and widths of these bars are proportional to the thickness of the tephra layers within the core, respectively.

Text SI4: Lake Ohrid chronological details

The chronology for the upper 247.8 m of core 5045-1 is that generated by Francke et al. (2016), and modified by Wagner et al. (2019) to cover the full 447 m succession (~1.36-Myr). To generate this chronology, tephrochronological data were used as first-order tie points (**Table S4**), but only in cases in which distinctive major element compositions or trace element datasets (see Leicher et al., 2016; Wagner et al., 2019) permitted unambiguous tephrostratigraphic correlations. A total of 16 tephra and cryptotephra layers were used in age-model generation for 5045-1. Tuning of climate-sensitive proxy data such as TOC and TIC (~480-year resolution) against orbital parameters were used to generate second-order tie points. Several TOC minima in Lake Ohrid coincide with times of the perihelion passage in March (Francke et al., 2016), which correspond to the points of greater winter season length at the latitude of Lake Ohrid (41° N). Increases in the length of the winter season collectively improve lake-water mixing that enhances oxidation of organic matter, resulting in moderate organic matter supply to the sediments and improved oxidation of organic matter at the sediment surface – signalled by minima in TOC that can be used for chronological tuning (Wagner et al., 2019). This orbital tuning approach yielded 66 second-order tie points for use in age-model generation, with estimated error margins of ±2-kyr. The independent chronological information obtained from tephrochronology and orbital tuning were cross-evaluated by the two palaeomagnetic age constraints: (1) the base of the Jaramillo sub-Chron boundary, and (2) the base of the Matuyama/Brunhes boundary.

The final age model was calculated using Bacon 2.269, considering broadly uniform sedimentation rates at the DEEP core site (Wagner et al., 2019). The average errors for specific depths averaged ±5.5-kyr (95% confidence), with a maximum uncertainty of ±10.68-kyr. The resulting chronology suggests that the upper 447.12 m of the DEEP site record continuously covers the past 1.35 Myr, and shows consistency (within errors) with U/Th-dated speleothem records from the Eastern Mediterranean (Bar-Matthews et al., 2003), and arboreal pollen percentages from the ~1.4-Myr Tenaghi Philippon record from northeast Greece (Tzedakis et al., 2006)

Table S3: Details of the tephra units identified in the upper ~36 m of DEEP 5045-1 (Francke et al., 2019; Leicher et al., 2021, 2016). Visible tephra layers are described with bold text, and M refers to eruption magnitude.

5045-1 ID (Unit)	Source	Unit	M	Tephra Composition
OH-DP-0009	Somma-Vesuvius	AD472/512	4.0?	Trachyte-Phonolite-Phonotephrite
OH-DP-0015	Etna	FL	N/A	Trachyte/ Basaltic Trachyandesite
OH-DP-0016.9	Somma-Vesuvius	Avellino?	5.3?	

OH-DP-0027	Somma-Vesuvius	Mercato	6.1	Phonolite
OH-DP-0049	Campi Flegrei	LN1	N/A	Trachyte
OH-DP-0052	Campi Flegrei	LN2?	N/A	Trachyte
OH-DP-0115	Campi Flegrei	Y-3	6.0	Trachyte-Phonolite
OH-DP-0169	Campi Flegrei	Y-5	7.7	Trachyte-Phonolite

Table S4: Tie-points used in generation of the age model for the upper ~36 m of core 5045-1 from Lake Ohrid analysed in this study.

Lab ID	Age (2σ) (ka)	Error (2σ) (ka)	Core Depth (m)	Description	Technique	Ref.
Tephra layers						
OH-DP-0009	1.46	0.02	0.904	512 AD (Somma-Vesuvius)	Historical	Historical
OH-DP-0015	3.37	0.07	1.554	FL (Etna)	$^{40}Ar/^{39}Ar$	1
OH-DP-0027	8.53	0.10	2.773	Mercato (Somma-Vesuvius)	$^{40}Ar/^{39}Ar$	2
OH-DP-0049	14.75	0.52	4.917	LN1 (N/A)	$^{40}Ar/^{39}Ar$	3
OH-DP-0115	29.05	0.37	11.507	Y-3 (Campi Flegrei)	$^{40}Ar/^{39}Ar$	4
OH-DP-0169	39.85	0.12	16.933	Y-5 (Campi Flegrei)	$^{40}Ar/^{39}Ar$	5
Inflection points						
	17	2	2.89	919 W/m^2	Orbital tuning	6
	40.1	2	6.55	502 W/m^2	Orbital tuning	6
	65.6	2	10.55	495 W/m^2	Orbital tuning	6
	88.5	2	14.26	507 W/m^2	Orbital tuning	6

1 –(Satow et al., 2015), 2 –(Giaccio et al., 2013), 3 – (Petrosino et al., 2014), 4 – (Marra et al., 2009)5 - (Giaccio et al., 2017), 6 - (Wagner et al., 2019)

SUPPLEMENTARY DISCUSSION

SD1: Hg normalization
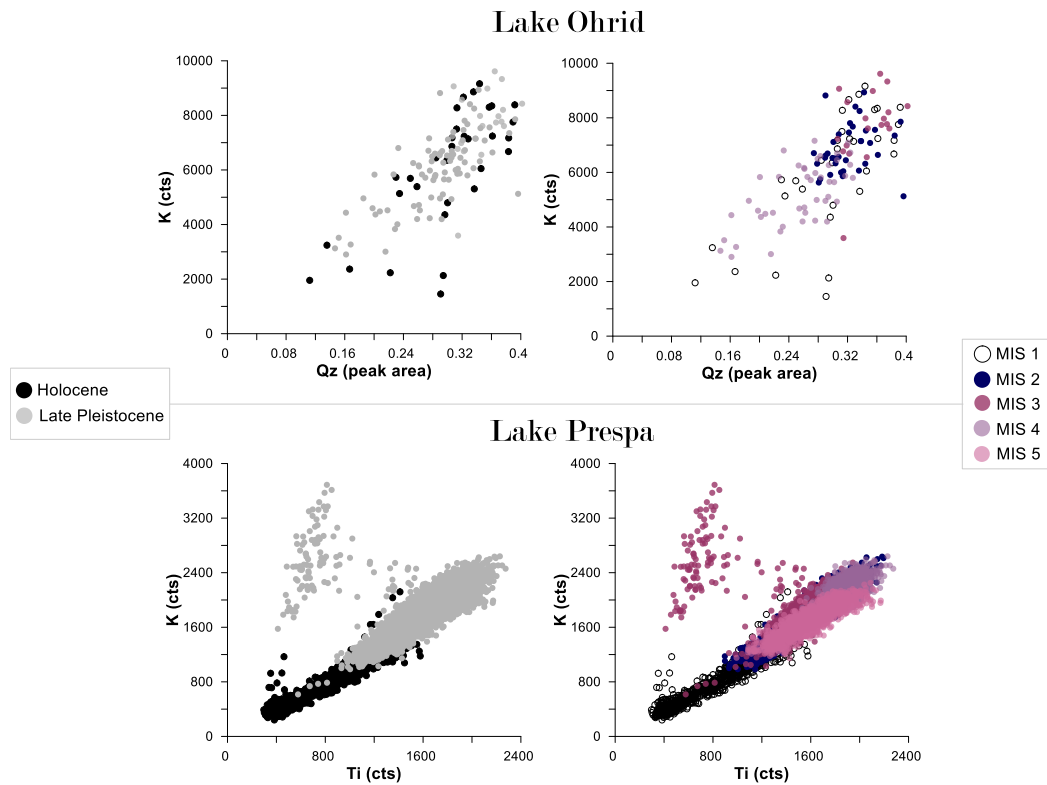
Figure S2: A comparison of geochemical relationships between detrital mineral proxies in lakes Prespa and Ohrid, with points colour-coded relative to stratigraphic period: the Holocene (12–0 ka, transparent circles), and the late Pleistocene (90–12 ka, filled circles). We compare potassium (K) records for both lakes relative to titanium (Ti) in Lake Prespa (Aufgebauer et al., 2012; Damaschke et al., 2013b), and to quartz (Qz) in Lake Ohrid (Francke et al., 2016; Wagner et al., 2019). We note that aluminium (Al) data are more commonly used as an indicator of detrital mineral abundance, but these are currently unavailable for 5045-1.
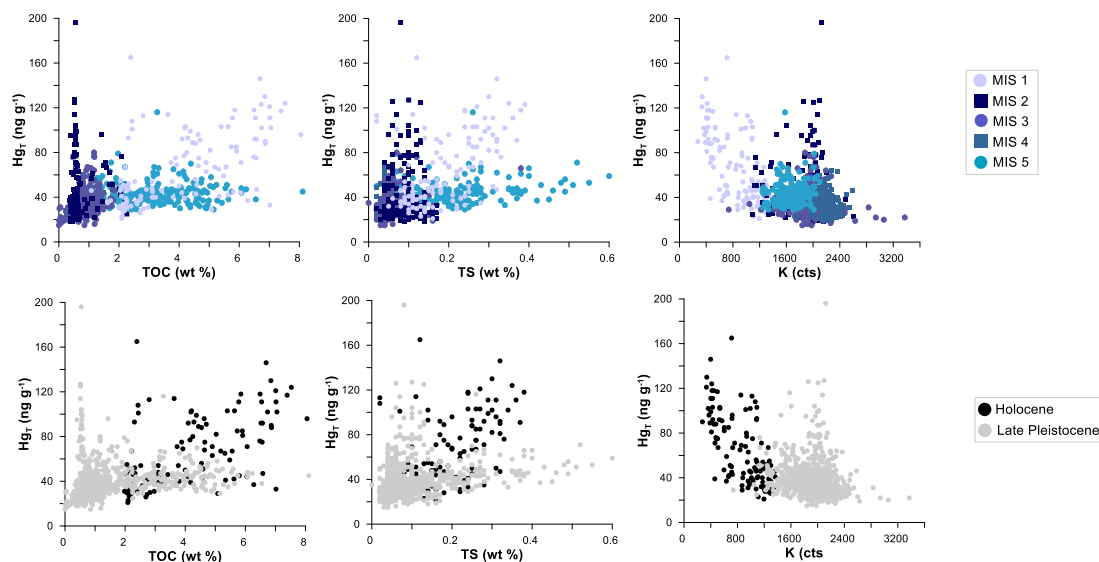
Figure S3: Total Hg (Hg_T) for Co1215 (Lake Prespa) plotted relative to total organic carbon (TOC), total sulfur (TS), total inorganic carbon (TIC), and potassium (K). TOC, TS, and K data for Co1215 generated by (Damaschke et al., 2013; Panagiotopoulos et al., 2014; Wagner et al., 2012). Data points are colour-coded based on time interval. We present the data first with respect to the Marine Isotope Stage (MIS) stratigraphic framework defined in Lisiecki & Raymo (2005)*, with stages defined as: MIS 5 – 130–71 ka; MIS 4 – 71–57 ka; MIS 3 – 57–29 ka; MIS 2 – 29–14 ka; MIS 1 – 14–0 ka. More broad stratigraphic boundaries are also considered: the Late Pleistocene (120 – 12 ka), and the Holocene (12–0 ka). We refer to the 'Late Pleistocene' (120–11 ka) and MIS 5 (130–71 ka) by their official chronological definitions, but also emphasize that the records presented here do not surpass ~100 ka in age.
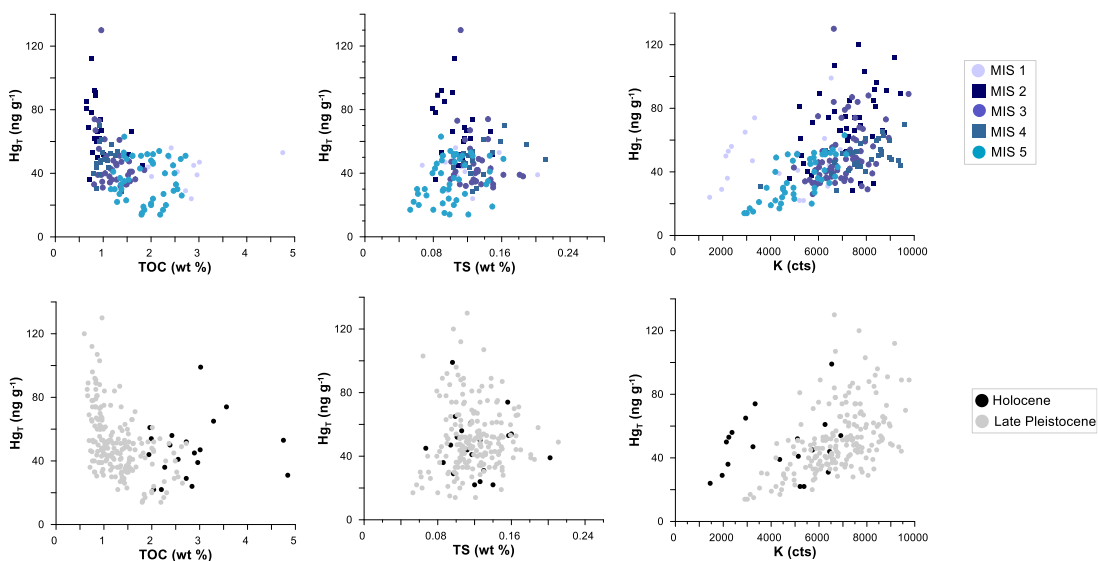
Figure S4: Total Hg (Hg_T) for 5045-1 (Lake Ohrid) plotted relative to total organic carbon (TOC), total sulfur (TS), total inorganic carbon (TIC), and potassium (K). TOC, TS, and K data for 5045-1 generated by (Francke et al., 2016; Wagner et al., 2019). Data points are colour-coded based on time interval. We present the data first with respect to the Marine Isotope Stage (MIS) stratigraphic framework defined in Lisiecki & Raymo (2005)*, with stages defined as: MIS 5 – 130–71 ka; MIS 4 – 71–57 ka; MIS 3 – 57–29 ka; MIS 2 – 29–14 ka; MIS 1 – 14–0 ka. More broad stratigraphic boundaries are also considered: the Late Pleistocene (120 – 12 ka), and the Holocene (12–0 ka). We refer to the 'Late Pleistocene' (120–11 ka) and MIS 5 (130–71 ka) by their official chronological definitions, but also emphasize that the records presented here do not surpass ~100 ka in age.

Table S4: Comparison of host-phase relationships (presented as the r-squared (r^2) value) between Lake Prespa and Lake Ohrid. r^2 values marked in bold/italic signal that the linear relationships observed between Hg_T and each compound examined was negative.

Lake	Host	MIS	r^2 value
Prespa	Hg_T/TOC	1	0.3375
		2	0.0105
		3	0.1053
		4	0.1381
		5	*0.0002*
	Hg_T/TS	1	0.2511
		2	0.0007
		3	0.056
		4	0.0431
		5	0.0751
	Hg_T/K	1	*0.4418*
		2	*0.0184*
		3	*0.0024*
		4	*0.031*
		5	0.0109
Ohrid	Hg_T/TOC	1	0.019
		2	*0.1495*
		3	*0.1477*
		4	*0.0293*
		5	*0.0004*
	Hg_T/TS	1	*0.007*
		2	*0.0367*
		3	*0.0074*
		4	0.1197
		5	0.0805
	Hg_T/K	1	0.0287
		2	0.1574
		3	0.1403
		4	0.3248
		5	0.5239

Text SD2: Early diagenetic processes

Variability in sedimentary Hg content may also be driven by (a)biotic processes occurring during, or shortly after deposition during early diagenesis. Several processes regulate Hg exchange between upper sediment layers and water column, for example by (de)methylation and formation of elemental Hg, and exchange of Hg between the surface waters and atmosphere (e.g., Rydberg et al., 2008). Redox changes are recognised in the Prespa and Ohrid records as evidence of authigenic carbonate formation, and so the ambient oxygen content of the water column and sediment pore-waters could modulate sedimentary Hg and normalised Hg (Hg/TOC, Hg/TS, Hg/Al). However, oscillations in Hg_T and Hg_{AR} do not correspond to measurable geochemical changes when examined relative to the authigenic carbonates, suggesting that Hg sequestration was not noticeably affected by the redox conditions that resulted in carbonate precipitation in Lake Ohrid or Lake Prespa.

Peaks in Hg_T do not coincide with the largest peaks in TIC, Mn/Ti, or Fe/Ti in Co1215. These elements manifest as layers or nodules of manganese (Mn) and iron (Fe) carbonates (mostly

siderite), indicating recurrent shifts in redox conditions or halted redox front migration and so provide evidence for reducing conditions and/or methanogenesis (Aufgebauer et al., 2012; Leng et al., 2013; Wagner et al., 2010). These ambient redox conditions can simultaneously influence the sedimentary Hg record, as Hg might be sequestered more effectively during strongly sulfidic conditions (as inclusions in pyrite or HgS; (Shen et al., 2020)) or evade sediments as methylated Hg (e.g. (Emili et al., 2011; Frieling et al., 2023). Indeed, temporary enrichments in Hg often appear in association with Fe and Mn around active redox fronts (Tribovillard et al., 2006; Mikac et al., 1999), and preservation (halting) of (paleo) redox fronts appear to influence Hg_T and normalized Hg measurements (Mercone et al., 1999; Frieling et al., 2023). However, instead a general decoupling is observed between Hg and these parameters in Lake Prespa.

The absence of coeval changes in Hg_T and Hg_{AR} with geochemical indicators of redox change also suggest that Hg burial in Lake Ohrid was not clearly affected by redox conditions. The 5045-1 core records distinct redox shifts coinciding with peaks in TIC, and interpreted as reflections of lake productivity and endogenic calcite dissolution (Wagner et al., 2009; Vogel et al., 2010; Francke et al., 2016). For example, calcite deposits are mainly concentrated in core sections characterised by high TIC and moderate Fe, whereas sections containing low TIC contain discrete horizons of siderite formation and Fe-enrichment, and it is likely that siderite formed during intervals characterised by rapid changes in sedimentation regime and/or bottom water redox conditions (Lacey et al., 2016; Vogel et al., 2010). The absence of distinct Hg signals coinciding with these redox shifts, therefore, suggest they did not significantly influence the sequestration of this compound during the interval of interest in this study.

Text SD2: Explosive volcanism

Variable Hg concentrations in Lakes Prespa and Ohrid cannot be unequivocally linked to explosive volcanism between ~90–0 ka (**Fig. S4**). The environmental impacts of explosive volcanism can be considered on two discrete timescales: (1) short-lived (<1-year) individual eruption events, and (2) long-term (>10^2-year) changes in eruption frequency. We explore potential reasons for our null result with respect to these two timescales below.

First, we considered individual eruption events. Explosive eruptions release prodigious amounts of pyroclastic material over geologically short timescales (<1-year), so the discrete ash layers preserved in lake sediment successions can provide precise stratigraphic markers for these events. Studies have hypothesized that volcanic Hg emissions may produce similarly transient, but nonetheless measurable, stratigraphic signals (Daga et al., 2016; Guédron et al., 2019; Ribeiro Guevara et al., 2010). SE Europe is home to a large number of active volcanoes with known activity during the Late Quaternary (Tomlinson et al., 2015). However, discrete ash fall events do not consistently correspond to measurable peaks in Hg concentration in our records. This is clearly observed in Lake Prespa where, despite a resolution of <100-years per sample, only two of the eleven preserved ash layers coincide with distinct peaks in Hg_T. These two units are not associated with disproportionately large tephra volumes and neither coincide with transient changes in carbonate precipitation/sediment

diagenesis, so no known mechanism can currently justify a causal link between these two layers; but not the other nine. It is even more difficult to assess the influence of individual eruption events on the Hg composition of the Lake Ohrid Hg record, as it is considerably coarser in resolution (~1000-yr per sample).
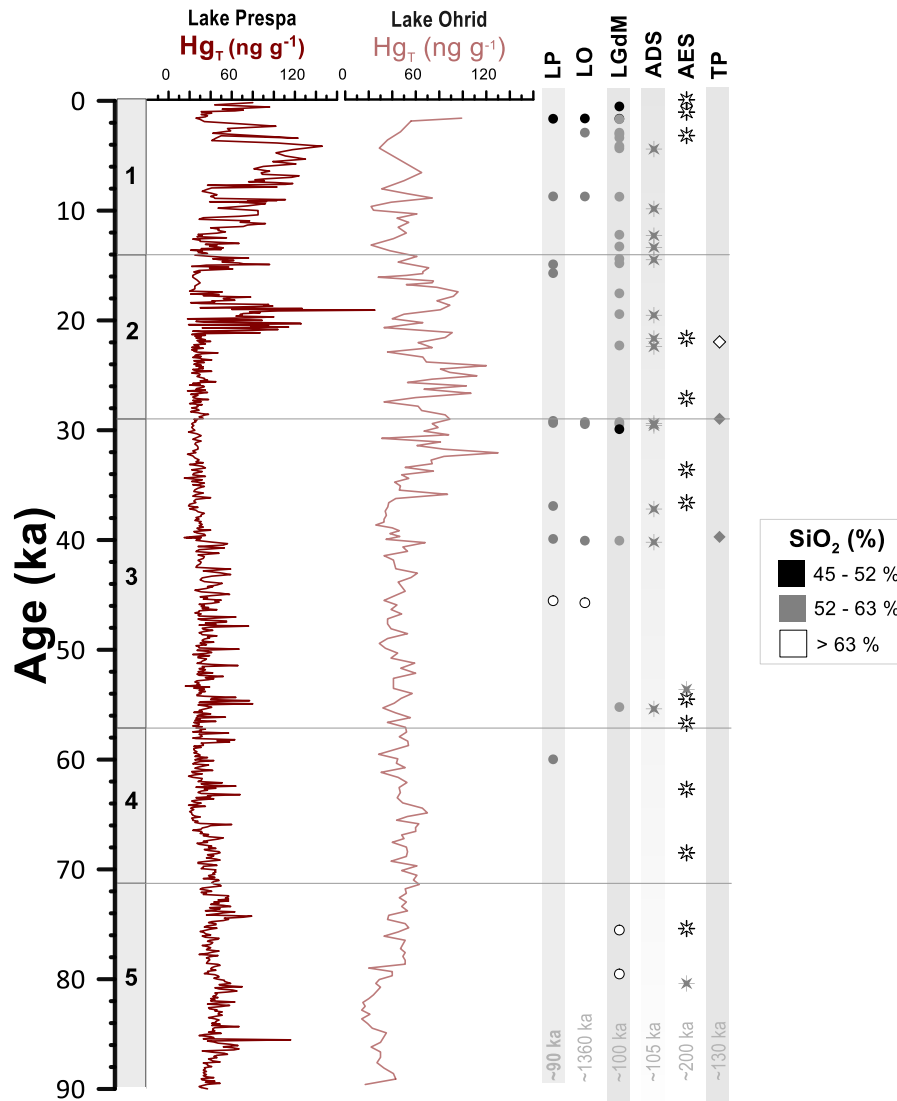
Figure S5: Time-resolved total Hg (Hg$_T$) data for Lake Prespa (Co1215) and Lake Ohrid (5045-1) compared to the number (n) and timing of eruptions identified using ash layers preserved in lacustrine successions (circles): Lake Prespa (LP) (Damaschke et al., 2013), Lake Ohrid (LO) (Leicher et al., 2021), and Lago Grande di Monticchio (LGdM) (Wulf et al., 2004), ocean sediment records (stars): the Adriatic (ADS) (Bourne et al., 2010) and Aegean (AES) (Kutterolf et al., 2021) seas, and peatland successions (diamonds): Tenaghi Phillippon (TP) (Wulf et al., 2018). The total temporal scope of each tephrostratigraphy is labelled in grey, and Marine Isotope Stages 1-5 are marked.

Next, we considered long-term changes in eruption frequency. Of the 53 SE European eruptions identified between ~90–0 ka, 62% occurred between 30–0 ka. This interval coincides with one of high Hg$_T$ and Hg$_{AR}$ in both Lake Prespa and Lake Ohrid (**Fig. S7**). This could be an artefact of discovery potential, given the greater number of Holocene-range lacustrine records available and/or better

characterization of younger tephra units in SE Europe. However, we note higher mean Hg_T and Hg_{AR} during MIS 1 and 2: intervals with a higher eruption frequency (**Table S4**). It has been speculated that measurable, millennial-scale changes in terrestrial Hg flux may occur during periods of elevated volcanic activity, owing to increases in the global atmospheric Hg load (Fadina et al., 2019; de Lacerda et al., 2017). We cannot rule out the possibility that increased Hg accumulation and deposition in lakes Prespa and Ohrid reflect a broad rise in regional volcanogenic Hg emissions. However, we equally cannot exclude the possibility that this observation is linked to better regional volcanic records for the Holocene, and/or a general rise in Hg emission from alternative sources (e.g., industrial practices) with our records alone.

Table S4: A comparison of the four marine isotope stages (MIS) relative to the number and frequency of eruptions considered in this study*, and mean Hg_T and Hg_{AR} values for Lake Prespa (LP) and Lake Ohrid (LO).

MIS	Interval (ka)	Eruptions (n)	Eruptions (n/1000 yr)	Mean Hg_T (ng g^{-1})		Mean Hg_{AR} (mg m^{-2} kyr^{-1})	
				LP	LO	LP	LO
1	14 – 0	18	1.29	64.64	47.2	34.72	26.23
2	29 – 14	12	1.09	41.91	69.23	16.44	45.47
3	57 – 29	2	0.15	32.84	50.57	8.99	33.41
4	71 – 57	4	0.29	33.67	50.15	10.39	29.62
5	130 - 71	6	0.12	44.21	36.02	13.34	20.38

* Eruptions are identified by their associated ash layers in cores sourced from Lakes Prespa (Damaschke et al., 2013), Ohrid (Leicher et al., 2016), Shkodra (Sulpizio et al., 2010), Lago Grande di Monticchio (Wulf et al., 2004), the Adriatic (Bourne et al., 2010) and Aegean (Kutterolf et al., 2021) seas, and the Tenaghi Phillippon (Wulf et al., 2018) peatland, and so the eruption counts given here do not represent the total number of global eruptions for the interval considered: rather the number of eruptions whose ash plumes were dispersed over the southeast Europe with an easterly trajectory. We also note that because eruption identification is reliant on preservation of a measurable ash layer within the sediment, these values are likely to underestimate the true number of eruptions affecting the region.

Two factors could explain the absence of clear volcanogenic Hg signals in the sediments of Lake Prespa and Lake Ohrid. First, that the dose of Hg delivered to the lake by a single eruption or dispersal mechanism was too low to produce a measurable signal. For example, reviews of published data suggest that the leachable Hg content is generally below the sedimentary detection limit (Ayris and Delmelle, 2012; Witham et al., 2005; Stewart et al., 2020). This is despite potential differences in Hg adsorption onto ash as a function of eruption style (Marumoto et al., 2017; Ohki et al., 2016), and suggests that the amount of Hg adsorbed onto ash particles may be insufficient to produce a distinguishable signal. The second factor is the decoupling between Hg and changes in authigenic carbonate content (**Text SD3: Early diagenetic processes**); which would negate production of a Hg signal in response to a change in Hg drawdown due to the leaching of other reactive compounds from the ash. This also underscores the importance lake-specific processes. Even if volcanic-induced perturbations to the local Hg cycle were sufficiently large to produce a measurable trace, signals

could be easily overprinted by local Hg inputs and/or sedimentary processes in the years following the eruption; effectively 'masking' any short-term perturbations in the Hg cycle. Assuming the eruptions in **Fig. S4** did release significant quantities of Hg, identification of an associated sedimentary signal would require that the enrichment from these emissions remain significant when averaged over the centuries that are represented by each sample; even for high-resolution cores such as Co1215 (~100 years). Temporal resolution and time-averaging are fundamental considerations for the identification of volcanic Hg emissions using sedimentary records, and our work suggests that sampling resolution would need to be significantly higher and/or focused on non-bioturbated records to have better prospect of identifying volcanogenic perturbations of the scale and type that may be present in the Ohrid and Prespa sedimentary successions.

References Cited

Albert, P. G., Hardiman, M., Keller, J., Tomlinson, E. L., Smith, V. C., Bourne, A. J., Wulf, S., Zanchetta, G., Sulpizio, R., Müller, U. C., Pross, J., Ottolini, L., Matthews, I. P., Blockley, S. P. E., and Menzies, M. A.: Revisiting the Y-3 tephrostratigraphic marker: A new diagnostic glass geochemistry, age estimate, and details on its climatostratigraphical context, Quaternary Science Reviews, 118, 105–121, https://doi.org/10.1016/j.quascirev.2014.04.002, 2015.

Aufgebauer, A., Panagiotopoulos, K., Wagner, B., Schaebitz, F., Viehberg, F. A., Vogel, H., Zanchetta, G., Sulpizio, R., Leng, M. J., and Damaschke, M.: Climate and environmental change in the Balkans over the last 17 ka recorded in sediments from Lake Prespa (Albania/F.Y.R. of Macedonia/Greece), Quaternary International, 274, 122–135, https://doi.org/10.1016/j.quaint.2012.02.015, 2012.

Ayris, P. M. and Delmelle, P.: The immediate environmental effects of tephra emission, Bulletin of Volcanology, 74, 1905–1936, https://doi.org/10.1007/s00445-012-0654-5, 2012.

Bar-Matthews, M., Ayalon, A., Gilmour, M., Matthews, A., and Hawkesworth, C. J.: Sea - land oxygen isotopic relationships from planktonic foraminifera and speleothems in the Eastern Mediterranean region and their implication for paleorainfall during interglacial intervals, Geochimica et Cosmochimica Acta, 67, 3181–3199, https://doi.org/10.1016/S0016-7037(02)01031-1, 2003.

Blaauw, M. and Christeny, J. A.: Flexible paleoclimate age-depth models using an autoregressive gamma process, Bayesian Analysis, 6, 457–474, https://doi.org/10.1214/11-BA618, 2011.

Bourne, A. J., Lowe, J. J., Trincardi, F., Asioli, A., Blockley, S. P. E., Wulf, S., Matthews, I. P., Piva, A., and Vigliotti, L.: Distal tephra record for the last ca 105,000 years from core PRAD 1-2 in the central Adriatic Sea: Implications for marine tephrostratigraphy, Quaternary Science Reviews, 29, 3079–3094, https://doi.org/10.1016/j.quascirev.2010.07.021, 2010.

Bronk Ramsey, C., Albert, P. G., Blockley, S. P. E., Hardiman, M., Housley, R. A., Lane, C. S., Lee, S., Matthews, I. P., Smith, V. C., and Lowe, J. J.: Improved age estimates for key Late Quaternary European tephra horizons in the RESET lattice, Quaternary Science Reviews, 118, 18–32, https://doi.org/10.1016/j.quascirev.2014.11.007, 2015.

Cheng, H., Edwards, R. L., Sinha, A., Spötl, C., Yi, L., Chen, S., Kelly, M., Kathayat, G., Wang, X., Li, X., Kong, X., Wang, Y., Ning, Y., and Zhang, H.: The Asian monsoon over the past 640,000 years and ice age terminations, Nature, 534, 640–646, https://doi.org/10.1038/nature18591, 2016.

Daga, R., Ribeiro Guevara, S., Pavlin, M., Rizzo, A., Lojen, S., Vreča, P., Horvat, M., and Arribére, M.: Historical records of mercury in southern latitudes over 1600 years: Lake Futalaufquen, Northern Patagonia, Science of the Total Environment, 553, 541–550, https://doi.org/10.1016/j.scitotenv.2016.02.114, 2016.

Damaschke, M., Sulpizio, R., Zanchetta, G., Wagner, B., Böhm, A., Nowaczyk, N., Rethemeyer, J., and Hilgers, A.: Tephrostratigraphic studies on a sediment core from Lake Prespa in the Balkans, Climate of the Past, 9, 267–287, https://doi.org/10.5194/cp-9-267-2013, 2013a.

Damaschke, M., Sulpizio, R., Zanchetta, G., Wagner, B., Böhm, A., Nowaczyk, N., Rethemeyer, J., and Hilgers, A.: Tephrostratigraphic studies on a sediment core from Lake Prespa in the Balkans, Climate of the Past, 9, 267–287, https://doi.org/10.5194/cp-9-267-2013, 2013b.

Damaschke, M., Sulpizio, R., Zanchetta, G., Wagner, B., Böhm, A., Nowaczyk, N., Rethemeyer, J., and Hilgers, A.: Tephrostratigraphic studies on a sediment core from Lake Prespa in the Balkans, Climate of the Past, 9, 267–287, https://doi.org/10.5194/cp-9-267-2013, 2013c.

Emili, A., Koron, N., Covelli, S., Faganeli, J., Acquavita, A., Predonzani, S., and Vittor, C. De: Does anoxia affect mercury cycling at the sediment-water interface in the Gulf of Trieste (northern Adriatic Sea)? Incubation experiments using benthic flux chambers, Applied Geochemistry, 26, 194–204, https://doi.org/10.1016/j.apgeochem.2010.11.019, 2011.

Fadina, O. A., Venancio, I. M., Belem, A., Silveira, C. S., Bertagnolli, D. de C., Silva-Filho, E. V., and Albuquerque, A. L. S.: Paleoclimatic controls on mercury deposition in northeast Brazil since the Last Interglacial, Quaternary Science Reviews, 221, 105869, https://doi.org/10.1016/j.quascirev.2019.105869, 2019.

Francke, A., Wagner, B., Just, J., Leicher, N., Gromig, R., Baumgarten, H., Vogel, H., Lacey, J. H., Sadori, L., Wonik, T., Leng, M. J., Zanchetta, G., Sulpizio, R., and Giaccio, B.: Sedimentological processes and environmental variability at Lake Ohrid (Macedonia, Albania) between 637 ka and the present, Biogeosciences, 13, 1179–1196, https://doi.org/10.5194/bg-13-1179-2016, 2016.

Francke, A., Dosseto, A., Panagiotopoulos, K., Leicher, N., Lacey, J. H., Kyrikou, S., Wagner, B., Zanchetta, G., Kouli, K., and Leng, M. J.: Sediment residence time reveals Holocene shift from climatic to vegetation control on catchment erosion in the Balkans, Global and Planetary Change, 177, 186–200, https://doi.org/10.1016/j.gloplacha.2019.04.005, 2019.

Frieling, J., Mather, T. A., März, C., Jenkyns, H. C., Hennekam, R., Reichart, G.-J., Slomp, C. P., and Van Helmond, N. A. G. M.: Effects of redox variability and early diagenesis on marine sedimentary Hg records, Geochimica et Cosmochimica Acta, S0016703723001850, https://doi.org/10.1016/j.gca.2023.04.015, 2023.

Giaccio, B., Arienzo, I., Sottili, G., Castorina, F., Gaeta, M., Nomade, S., Galli, P., and Messina, P.: Isotopic (Sr–Nd) and major element fingerprinting of distal tephras: an application to the Middle-Late Pleistocene markers from the Colli Albani volcano, central Italy, Quaternary Science Reviews, 67, 190–206, https://doi.org/10.1016/j.quascirev.2013.01.028, 2013.

Giaccio, B., Hajdas, I., Isaia, R., Deino, A., and Nomade, S.: High-precision 14C and 40Ar/39 Ar dating of the Campanian Ignimbrite (Y-5) reconciles the time-scales of climatic-cultural processes at 40 ka, Scientific Reports, 7, 1–10, https://doi.org/10.1038/srep45940, 2017.

Guédron, S., Tolu, J., Brisset, E., Sabatier, P., Perrot, V., Bouchet, S., Develle, A. L., Bindler, R., Cossa, D., Fritz, S. C., and Baker, P. A.: Late Holocene volcanic and anthropogenic mercury deposition in the western Central Andes (Lake Chungará Chile), Science of the Total Environment, 662, 903–914, https://doi.org/10.1016/j.scitotenv.2019.01.294, 2019.

Hughen, K. A. and Heaton, T. J.: Updated Cariaco Basin 14C Calibration Dataset from 0–60 cal kyr BP, Radiocarbon, 62, 1001–1043, https://doi.org/10.1017/RDC.2020.53, 2020.

Kutterolf, S., Freundt, A., Hansteen, T. H., Dettbarn, R., Hampel, F., Sievers, C., Wittig, C., Allen, S. R., Druitt, T. H., McPhie, J., Nomikou, P., Pank, K., Schindlbeck-Belo, J. C., Wang, K. L., Lee, H. Y., and Friedrichs, B.: The Medial Offshore Record of Explosive Volcanism Along the Central to Eastern Aegean Volcanic Arc: 1. Tephrostratigraphic Correlations, Geochemistry, Geophysics, Geosystems, 22, https://doi.org/10.1029/2021GC010010, 2021.

de Lacerda, L. D., Turcq, B., Sifeddine, A., and Cordeiro, R. C.: Mercury accumulation rates in Caço Lake, NE Brazil during the past 20.000 years, Journal of South American Earth Sciences, 77, 42–50, https://doi.org/10.1016/j.jsames.2017.04.008, 2017.

Lacey, J. H., Leng, M. J., Francke, A., Sloane, H. H., Milodowski, A., Vogel, H., Baumgarten, H., Zanchetta, G., and Wagner, B.: Northern Mediterranean climate since the Middle Pleistocene: A 637 ka stable isotope record from Lake Ohrid (Albania/Macedonia), Biogeosciences, 13, 1801–1820, https://doi.org/10.5194/bg-13-1801-2016, 2016.

Leicher, N., Zanchetta, G., Sulpizio, R., Giaccio, B., Wagner, B., Nomade, S., Francke, A., and Del Carlo, P.: First tephrostratigraphic results of the DEEP site record from Lake Ohrid (Macedonia and Albania), Biogeosciences, 13, 2151–2178, https://doi.org/10.5194/bg-13-2151-2016, 2016.

Leicher, N., Giaccio, B., Zanchetta, G., Sulpizio, R., Albert, P. G., Tomlinson, E. L., Lagos, M., Francke, A., and Wagner, B.: Lake Ohrid's tephrochronological dataset reveals 1.36 Ma of Mediterranean explosive volcanic activity, Scientific Data, 8, 1–14, https://doi.org/10.1038/s41597-021-01013-7, 2021.

Leng, M. J., Wagner, B., Boehm, A., Panagiotopoulos, K., Vane, C. H., Snelling, A., Haidon, C., Woodley, E., Vogel, H., Zanchetta, G., and Baneschi, I.: Understanding past climatic and hydrological variability in the mediterranean from Lake Prespa sediment isotope and geochemical record over the last glacial cycle, Quaternary Science Reviews, 66, 123–136, https://doi.org/10.1016/j.quascirev.2012.07.015, 2013.

Marra, F., Karner, D. B., Freda, C., Gaeta, M., and Renne, P.: Large mafic eruptions at Alban Hills Volcanic District (Central Italy): Chronostratigraphy, petrography and eruptive behavior, Journal of Volcanology and Geothermal Research, 179, 217–232, https://doi.org/10.1016/j.jvolgeores.2008.11.009, 2009.

Marumoto, K., Sudo, Y., and Nagamatsu, Y.: Collateral variations between the concentrations of mercury and other water soluble ions in volcanic ash samples and volcanic activity during the 2014–2016 eruptive episodes at Aso volcano, Japan, Journal of Volcanology and Geothermal Research, 341, 149–157, https://doi.org/10.1016/j.jvolgeores.2017.05.022, 2017.

Mercone, D., Thomson, J., Croudace, I. W., and Troelstra, S. R.: A coupled natural immobilisation mechanism for mercury and selenium in deep-sea sediments, Geochimica et Cosmochimica Acta, 63, 1481–1488, https://doi.org/10.1016/S0016-7037(99)00063-0, 1999.

Mikac, N., Niessen, S., Ouddane, B., and Wartel, M.: Speciation of mercury in sediments of the Seine estuary (France), Applied Organometallic Chemistry, 13, 715–725, https://doi.org/10.1002/(SICI)1099-0739(199910)13:10<715::AID-AOC918>3.0.CO;2-4, 1999.

Ohki, A., Nakajima, T., Hayashi, K., Taniguchi, H., Haraguchi, K., and Takanashi, H.: Levels of Hg and other chemical elements in volcanic ash fall samples erupted from Mt. Sakurajima, Japan, Toxicological and Environmental Chemistry, 98, 778–786, https://doi.org/10.1080/02772248.2016.1139117, 2016.

Panagiotopoulos, K., Böhm, A., Leng, M. J., Wagner, B., and Schäbitz, F.: Climate variability over the last 92 ka in SW Balkans from analysis of sediments from Lake Prespa, Climate of the Past, 10, 643–660, https://doi.org/10.5194/cp-10-643-2014, 2014.

Petrosino, P., Jicha, B. R., Mazzeo, F. C., and Russo Ermolli, E.: A high resolution tephrochronological record of MIS 14–12 in the Southern Apennines (Acerno Basin, Italy), Journal of Volcanology and Geothermal Research, 274, 34–50, https://doi.org/10.1016/j.jvolgeores.2014.01.014, 2014.

Ramsey, C. B.: Bayesian analysis of radiocarbon dates, Radiocarbon, 51, 337–360, https://doi.org/10.1017/s0033822200033865, 2009.

Reimer, P., Baillie, M. G. L., Bard, E., Bayliss, A., Beck, J. W., Blackwell, P. G., Bronk-Ramsey, C., Buck, C. E., Burr, G. S., Edwards, R. L., Friedrich, M., Grootes, P. M., Guilderson, T. P., Hajdas, I., Heaton, T. J., Hogg, A. G., Hughen, K. A., Kaiser, K. F., Kromer, B., McCormac, F. G., Manning, S. W., Reimer, R. W., Richards, D. A., Southon, J. R., Talamo, S., Turney, C. S. M., van der Plicht, J., and Weyhenmeyer, C. E.: INTCAL09 and MARINE09 radiocarbon age calibration curves 0–50000 years cal BP, Radiocarbon, 51, 1111–1150, 2009.

Reimer, P. J., Austin, W. E. N., Bard, E., Bayliss, A., Blackwell, P. G., Bronk Ramsey, C., Butzin, M., Cheng, H., Edwards, R. L., Friedrich, M., Grootes, P. M., Guilderson, T. P., Hajdas, I., Heaton, T. J., Hogg, A. G., Hughen, K. A., Kromer, B., Manning, S. W., Muscheler, R., Palmer, J. G., Pearson, C., Van Der Plicht, J., Reimer, R. W., Richards, D. A., Scott, E. M., Southon, J. R., Turney, C. S. M., Wacker, L., Adolphi, F., Büntgen, U., Capano, M., Fahrni, S. M., Fogtmann-Schulz, A., Friedrich, R., Köhler, P., Kudsk, S., Miyake, F., Olsen, J., Reinig, F., Sakamoto, M., Sookdeo, A., and Talamo, S.: The IntCal20 Northern Hemisphere Radiocarbon Age Calibration Curve (0-55 cal kBP), Radiocarbon, 62, 725–757, https://doi.org/10.1017/RDC.2020.41, 2020.

Ribeiro Guevara, S., Meili, M., Rizzo, A., Daga, R., and Arribére, M.: Sediment records of highly variable mercury inputs to mountain lakes in patagonia during the past millennium, Atmospheric Chemistry and Physics, 10, 3443–3453, https://doi.org/10.5194/acp-10-3443-2010, 2010.

Rydberg, J., Gälman, V., Renberg, I., Bindler, R., Lambertsson, L., and Martínez-Cortizas, A.: Assessing the stability of mercury and methylmercury in a varved lake sediment deposit, Environmental Science and Technology, 42, 4391–4396, https://doi.org/10.1021/es7031955, 2008.

Satow, C., Tomlinson, E. L., Grant, K. M., Albert, P. G., Smith, V. C., Manning, C. J., Ottolini, L., Wulf, S., Rohling, E. J., Lowe, J. J., Blockley, S. P. E., and Menzies, M. A.: A new contribution to the Late Quaternary tephrostratigraphy of the Mediterranean: Aegean Sea core LC21, Quaternary Science Reviews, 117, 96–112, https://doi.org/10.1016/j.quascirev.2015.04.005, 2015.

Shen, J., Feng, Q., Algeo, T. J., Liu, J., Zhou, C., Wei, W., Liu, J., Them, T. R., Gill, B. C., and Chen, J.: Sedimentary host phases of mercury (Hg) and implications for use of Hg as a volcanic proxy, Earth and Planetary Science Letters, 543, 116333, https://doi.org/10.1016/j.epsl.2020.116333, 2020.

Staff, R. A., Nakagawa, T., Schlolaut, G., Marshall, M. H., Brauer, A., Lamb, H. F., Bronk Ramsey, C., Bryant, C. L., Brock, F., Kitagawa, H., Van der Plicht, J., Payne, R. L., Smith, V. C., Mark, D. F., Macleod, A., Blockley, S. P. E., Schwenninger, J. L., Tarasov, P. E., Haraguchi, T., Gotanda, K., Yonenobu, H., and Yokoyama, Y.: The multiple chronological techniques applied to the Lake Suigetsu SG06 sediment core, central Japan, Boreas, 42, 259–266, https://doi.org/10.1111/j.1502-3885.2012.00278.x, 2013.

Stewart, C., Damby, D. E., Tomašek, I., Horwell, C. J., Plumlee, G. S., Armienta, M. A., Hinojosa, M. G. R., Appleby, M., Delmelle, P., Cronin, S., Ottley, C. J., Oppenheimer, C., and Morman, S.: Assessment of leachable elements in volcanic ashfall: a review and evaluation of a standardized protocol for ash hazard characterization, Journal of Volcanology and Geothermal Research, 392, https://doi.org/10.1016/j.jvolgeores.2019.106756, 2020.

Sulpizio, R., Van Welden, A., Caron, B., and Zanchetta, G.: The Holocene tephrostratigraphic record of Lake Shkodra (Albania and Montenegro), Journal of Quaternary Science, 25, 633–650, https://doi.org/10.1002/jqs.1334, 2010.

Tomlinson, E. L., Smith, V. C., Albert, P. G., Aydar, E., Civetta, L., Cioni, R., Çubukçu, E., Gertisser, R., Isaia, R., Menzies, M. A., Orsi, G., Rosi, M., and Zanchetta, G.: The major and trace element glass compositions of the productive Mediterranean volcanic sources: Tools for correlating distal tephra layers in and around Europe, Quaternary Science Reviews, 118, 48–66, https://doi.org/10.1016/j.quascirev.2014.10.028, 2015.

Tribovillard, N., Algeo, T. J., Lyons, T., and Riboulleau, A.: Trace metals as paleoredox and paleoproductivity proxies: An update, Chemical Geology, 232, 12–32, https://doi.org/10.1016/j.chemgeo.2006.02.012, 2006.

Tzedakis, P. C., Hooghiemstra, H., and Pälike, H.: The last 1.35 million years at Tenaghi Philippon: revised chronostratigraphy and long-term vegetation trends, Quaternary Science Reviews, 25, 3416–3430, https://doi.org/10.1016/j.quascirev.2006.09.002, 2006.

Vogel, H., Wagner, B., Zanchetta, G., Sulpizio, R., and Rosén, P.: A paleoclimate record with tephrochronological age control for the last glacial-interglacial cycle from Lake Ohrid, Albania and Macedonia, Journal of Paleolimnology, 44, 295–310, https://doi.org/10.1007/s10933-009-9404-x, 2010.

Wagner, B., Lotter, A. F., Nowaczyk, N., Reed, J. M., Schwalb, A., Sulpizio, R., Valsecchi, V., Wessels, M., and Zanchetta, G.: A 40,000-year record of environmental change from ancient Lake Ohrid (Albania and Macedonia), Journal of Paleolimnology, 41, 407–430, https://doi.org/10.1007/s10933-008-9234-2, 2009.

Wagner, B., Vogel, H., Zanchetta, G., and Sulpizio, R.: Environmental change within the Balkan region during the past ca. 50 ka recorded in the sediments from lakes Prespa and Ohrid, Biogeosciences, 7, 3187–3198, https://doi.org/10.5194/bg-7-3187-2010, 2010.

Wagner, B., Aufgebauer, A., Vogel, H., Zanchetta, G., Sulpizio, R., and Damaschke, M.: Late Pleistocene and Holocene contourite drift in Lake Prespa (Albania/F.Y.R. of Macedonia/Greece), Quaternary International, 274, 112–121, https://doi.org/10.1016/j.quaint.2012.02.016, 2012.

Wagner, B., Wilke, T., Krastel, S., Zanchetta, G., Sulpizio, R., Reicherter, K., Leng, M., Grazhdani, A., Trajanovski, S., Levkov, Z., Reed, J., and Wonik, T.: More than one million years of history in Lake Ohrid cores, Eos, 95, 25–26, https://doi.org/10.1002/2014EO030001, 2014.

Wagner, B., Vogel, H., Francke, A., Friedrich, T., Donders, T., Lacey, J. H., Leng, M. J., Regattieri, E., Sadori, L., Wilke, T., Zanchetta, G., Albrecht, C., Bertini, A., Combourieu-Nebout, N., Cvetkoska, A., Giaccio, B., Grazhdani, A., Hauffe, T., Holtvoeth, J., Joannin, S., Jovanovska, E., Just, J., Kouli, K., Kousis, I., Koutsodendris, A., Krastel, S., Lagos, M., Leicher, N., Levkov, Z., Lindhorst, K., Masi, A., Melles, M., Mercuri, A. M., Nomade, S., Nowaczyk, N., Panagiotopoulos, K., Peyron, O., Reed, J. M., Sagnotti, L., Sinopoli, G., Stelbrink, B., Sulpizio, R., Timmermann, A., Tofilovska, S., Torri, P., Wagner-Cremer, F., Wonik, T., and Zhang, X.: Mediterranean winter rainfall in phase with African monsoons during the past 1.36 million years, Nature, 573, 256–260, https://doi.org/10.1038/s41586-019-1529-0, 2019.

Witham, C. S., Oppenheimer, C., and Horwell, C. J.: Volcanic ash-leachates: A review and recommendations for sampling methods, Journal of Volcanology and Geothermal Research, 141, 299–326, https://doi.org/10.1016/j.jvolgeores.2004.11.010, 2005.

Wulf, S., Kraml, M., Brauer, A., Keller, J., and Negendank, J. F. W.: Tephrochronology of the 100ka lacustrine sediment record of Lago Grande di Monticchio (southern Italy), Quaternary International, 122, 7–30, https://doi.org/10.1016/j.quaint.2004.01.028, 2004.

Wulf, S., Hardiman, M. J., Staff, R. A., Koutsodendris, A., Appelt, O., Blockley, S. P. E., Lowe, J. J., Manning, C. J., Ottolini, L., Schmitt, A. K., Smith, V. C., Tomlinson, E. L., Vakhrameeva, P., Knipping, M., Kotthoff, U., Milner, A. M., Müller, U. C., Christanis, K., Kalaitzidis, S., Tzedakis, P. C., Schmiedl, G., and Pross, J.: The marine isotope stage 1–5 cryptotephra record of Tenaghi Philippon, Greece: Towards a detailed tephrostratigraphic framework for the Eastern Mediterranean region, Quaternary Science Reviews, 186, 236–262, https://doi.org/10.1016/j.quascirev.2018.03.011, 2018.

Zanchetta, G., Giaccio, B., Bini, M., and Sarti, L.: Tephrostratigraphy of Grotta del Cavallo, Southern Italy: Insights on the chronology of Middle to Upper Palaeolithic transition in the Mediterranean, Quaternary Science Reviews, 182, 65–77, https://doi.org/10.1016/j.quascirev.2017.12.014, 2018.